Fatigue Reliability Analysis of Heavy-Haul Railway T-Beams Based on Miner's Rule and Point Estimation Method

Jianyu Zhang
College of Architecture and Civil Engineering, Beijing University of Technology, Beijing, China

Abstract: To clarify the fatigue failure law and reliability level of 32m prestressed concrete simply supported T-beams for heavy-haul railways, address the fatigue damage problem of such bridges caused by long-term alternating train loads, and consider the aggravating effect of prestress attenuation induced by concrete dynamic creep and prestressing tendon relaxation on fatigue risk, relevant research is carried out to provide theoretical support for fatigue safety assessment and operation maintenance in engineering practice. Taking the 32m prestressed concrete simply supported T-beam of heavy-haul railways as the research object, based on the Miner linear cumulative damage theory and material S-N curve, a fatigue limit state function considering prestress attenuation is established, and the corresponding fatigue limit state functions are respectively derived for three typical failure modes, namely concrete compressive failure, tensile cracking and reinforcement fatigue fracture. The influence of prestress attenuation should be included in the equivalent stress amplitude of the lower flange, while the equivalent stress amplitudes of the upper flange and steel bars are temporarily ignored due to their weak correlation with prestress attenuation. The point estimation method is adopted to calculate the time-varying fatigue reliability index of the bridge within its 100-year service life, and the influence of load parameters on the reliability evolution is analyzed. The results show that the fatigue failure probability of prestressed steel bars and upper flange concrete of 32m prestressed concrete simply supported T-beams for heavy-haul railways is low with sufficient safety margin; the initial reliability index of lower flange concrete is 4.885, which drops to 1.970 after 100 years of service, making it the key fatigue control part. The established limit state function and adopted analysis method can effectively quantify the fatigue safety level of such bridges and provide a scientific basis for design, assessment and maintenance.

Keywords: Heavy-Haul Railway; Prestressed Concrete Simply Supported T-Beam; Fatigue Reliability; Prestress Attenuation

1. Introduction

Heavy-haul railways serve as the core infrastructure for the transportation of national bulk commodities and act as vital corridors for the delivery of strategic materials such as energy resources and minerals[1,2]. Simply supported T-beams are widely adopted in heavy-haul railway bridges (predominantly the 32-meter standard span beams) due to their clear stress distribution, convenient construction and excellent economic efficiency. However, long-term exposure to alternating train loads tends to cause cumulative fatigue damage, and may even trigger brittle failure[3-5]. Meanwhile, concrete creep and prestressed tendon relaxation lead to continuous attenuation of effective prestress, alter the structural stress state, and aggravate the fatigue risk at key components such as the lower flange[6]. Therefore, conducting fatigue reliability analysis on prestressed simply-supported T-beams of heavy-haul railways holds important engineering significance for ensuring bridge service safety and extending service life.

Existing research has conducted extensive studies on the fatigue performance and reliability of prestressed concrete beams. In terms of fatigue damage theory and failure modes, the Miner's linear cumulative damage theory [7] serves as the core basis for variable amplitude fatigue evaluation, and SONSINO et al. [8] have improved the conversion method from variable amplitude loads to constant amplitude loads. Song et al. [9] identified three typical failure modes of simply supported T-beams in heavy-haul railways, namely concrete compressive failure, tensile cracking, and reinforcement fatigue fracture, and the tensile and compressive fatigue strength of concrete can be described by the S-N curve[10]. Yang Ou et al[11]. pointed out that the fatigue failure of PC beams mostly initiates from the fracture of stressed reinforcements, and the concrete in the compression zone generally does not suffer fatigue failure due to the small stress amplitude. This conclusion has been verified by fatigue tests on heavy-haul railway bridges [12,13]. In terms of reliability analysis methods, the point estimation method[14] has been applied to the efficient calculation of fatigue reliability of reinforced concrete beams for heavy-haul railways. Considering time-varying characteristics[15], scholars have established time-varying fatigue reliability models for steel bridges and adopted the PHI2 method[16] to analyze the time-varying crack resistance reliability of 32m simply supported T-beams. Regarding the influence of loads, studies[17] have shown that the increase in train axle load can significantly shorten the fatigue life of RC beams, and the vehicle-bridge coupling theory has also been used to quantify the influence of train loads on the stress amplitude of beam structures.

Although existing achievements have laid a theoretical foundation, there are still shortcomings: most studies have not systematically considered the influence of long-term prestress attenuation on the stress amplitude of the lower flange of simply supported T-beams, leading to overly optimistic reliability estimation; there is insufficient differentiated analysis of reliability at different structural parts, with most researches focusing only on beam reinforcement and lacking targeted quantification for the lower flange where fatigue risk is most concentrated; some studies have simplified the impact of actual train parameters on bridge stress amplitude.

Therefore, taking simply supported T-beams of heavy-haul railways as the research object, this paper establishes a fatigue limit state function considering prestress attenuation based on the Miner's rule and material S-N curve, with a focus on quantifying the response of the equivalent stress amplitude of the lower flange to prestress degradation. A method combining the point estimation method and Monte Carlo simulation is adopted to calculate the time-variant reliability indices of three typical failure modes. By comparing the reliability evolution laws of different components, the characteristic of low reliability of the lower flange is revealed. This study aims to fill the gap in relevant analysis, clarify the maintenance priority of the lower flange in the middle and later operation stages, and provide theoretical support for fatigue safety assessment and maintenance decision-making of simply supported T-beams in heavy-haul railways.

2. Establishment of Fatigue Limit State Function

2.2 Equivalent Constant Amplitude Fatigue for Variable Amplitude Fatigue Problem

Under cyclic loading, damage occurs to the internal materials of structures. With the continuous accumulation of damage, brittle failure may take place even when the structural stress level is lower than the material strength, which is referred to as fatigue failure in engineering.

For reinforced concrete bridges of heavy-haul railways, multiple failure modes exist under alternating loads, among which concrete compressive failure, tensile cracking and steel bar fatigue fracture are typical failure modes[1]. Therefore, this paper mainly analyzes these three failure modes.

According to the Miner fatigue damage theory[7], the fatigue damage to bridge structures caused by cyclic loads at all levels can be linearly accumulated. When the accumulated fatigue damage reaches the critical level (i.e., D=1), fatigue failure of the structure will occur. Hence, the fatigue limit state function of concrete bridges during the service period can be expressed as:

$$G\,[\mathbf{X},t] = 1 - D(t) \tag{1}$$

Among them, $D(t)$ denotes the cumulative fatigue damage of the bridge within the time interval [0,*t*], When $G\,[\mathbf{X},t] \le 0$, it indicates that the structure undergoes fatigue failure.

According to the Miner's rule, the damage caused by stresses at all levels can be expressed as:

$$D(t) = \sum_{i=1}^{k} \frac{n_i(t)}{N_i} \tag{2}$$

where D denotes the fatigue damage; k represents different stress levels; n_i is the number of stress cycles corresponding to the stress amplitude $\Delta\sigma_i$ According to Equation

(1), fatigue failure of the structure occurs when the cumulative fatigue damage $D(t)>1$ Therefore, the fatigue failure probability $P_f(T)$ of the bridge within the time interval [0,T] is given by:

$$P_f(T)=\Pr\{D(t)\geq 1,\exists t\in[0,T]\}=\Pr\left\{D(t)=\sum_{i=1}^{k}\frac{n_i}{N_i}\geq 1,\exists t\in[0,T]\right\} \quad (3)$$

For fatigue assessment under a single constant stress amplitude, the S-N method can be directly applied. The S-N curve defines the relationship between the constant-amplitude stress range induced by external loads and the corresponding number of stress cycles, which can be expressed as:

$$\lg N=\lg C-m\lg(\Delta\sigma) \quad (4)$$

where $\Delta\sigma_i=\sigma_{\max,i}-\sigma_{\min,i}$ is the constant stress amplitude; m and C are material fatigue performance parameters; N is the fatigue life under a specific stress amplitude.

However, in practical engineering, the train loads acting on heavy-haul railway bridges exhibit strong randomness (such as axle load fluctuations, train speed variations, track irregularities, etc.), resulting in that the stress amplitudes inside the structure are not constant values but time-varying variable-amplitude stress cycles (i.e., different stress amplitudes $\Delta\sigma_1,\Delta\sigma_2,\ldots\Delta\sigma_k$ act alternately). Therefore, the fatigue of concrete beams under train loads falls into the category of variable-amplitude fatigue. It is thus necessary to adopt the equivalent stress amplitude to replace the variable-amplitude stress ranges for analysis. The core of the equivalent stress amplitude method is the equivalence principle: the fatigue damage induced by the equivalent stress amplitude is equal to the total damage caused by all variable-amplitude stresses. Therefore, substituting the rearranged form of Equation (4) $N_i=C/\Delta\sigma_i^m$ into Equation (2) yields:

$$D(t)=\sum_{i=1}^{k}\frac{n_i\cdot\Delta\sigma_i^m}{C} \quad (5)$$

Let the fatigue strength of the material under *N*e cycles of constant-amplitude repeated stress over the time interval *t* be $\sigma_{\mathrm{R},N_\mathrm{e}}$. According to the S-N curve relationship of the material, it follows that $C=N_\mathrm{e}(\sigma_{\mathrm{R},N_\mathrm{e}})^m$, then:

$$D(t)=\sum_{i=1}^{k}\frac{n_i\cdot\Delta\sigma_i^m}{N_e\sigma_{\mathrm{R},N_\mathrm{e}}^m}=\frac{\sum_{i=1}^{k}n_i\,\Delta\sigma_i^m}{N_e\sigma_{\mathrm{R},N_\mathrm{e}}^m} \quad (6)$$

Let the probability density function of the structural stress level $\Delta\sigma_i$ be denoted as $f_{\Delta\sigma_i}(\Delta\sigma_i)$. For high-cycle fatigue, when the total number of cycles is sufficiently large (generally greater than 10^5). that is, when n approaches infinity and, $N_\mathrm{e}=\sum_{i=1}^{k}n_i$, the number of load cycles corresponding to the stress leve σ_i is given by $n_i(t)=N_\mathrm{e}f_{\Delta\sigma_i}\mathrm{d}(\Delta\sigma_i)$, Substituting this into Equation (6) and further deriving yields:

$$D(t)=\frac{\sum_{i=1}^{k}n_i\Delta\sigma_i^m}{N_e\sigma_{\mathrm{R}N_\mathrm{e}}^m}=\frac{\sum_{i=1}^{k}N_\mathrm{e}f_{\Delta\sigma_i}\Delta\sigma_i^m\mathrm{d}(\Delta\sigma_i)}{N_e\sigma_{\mathrm{R}N_\mathrm{e}}^m}=\int_0^{+\infty}\frac{N_\mathrm{e}f_{\Delta\sigma_i}\mathrm{d}(\Delta\sigma_i)}{N_e\sigma_{\mathrm{R}N_\mathrm{e}}^m}=\frac{E(\Delta\sigma^m)}{\sigma_{\mathrm{R}N_\mathrm{e}}^m} \quad (7)$$

where $\mathrm{E}(\cdot)$ denotes the mathematical expectation.

Substituting Equation (7) into Equation (3) yields:

$$P_f(T)=\Pr\{D(t)\geq 1,\exists t\in[0,T]\}=\Pr\{\frac{E(\Delta\sigma^m)}{\sigma_{\mathrm{R},N_\mathrm{e}}^m}\geq 1,\exists t\in[0,T]\}$$

$$\Rightarrow\Pr\{\sigma_{\mathrm{R},N_\mathrm{e}}<\left(E[(\Delta\sigma_i)^m]\right)^{\frac{1}{m}},\exists t\in[0,T]\} \quad (8)$$

Then, the fatigue limit state function can be expressed as:

$$G[\mathbf{X},t]=\sigma_{\mathrm{R}N_\mathrm{e}}-\sigma_\mathrm{e}=\sigma_{\mathrm{R}N_\mathrm{e}}-\left(E[(\Delta\sigma_i)^m]\right)^{\frac{1}{m}} \quad (9)$$

where $\sigma_{\mathrm{R},N_\mathrm{e}}$ is the fatigue strength under constant-amplitude repeated stress; σ_e represents the equivalent constant-amplitude stress corresponding to N_e cycles of cyclic loads under variable-amplitude loads; $\Delta\sigma_i$ represents the stress variation amplitude of the track slab under external loads; $\mathrm{E}(\cdot)$ denotes the mathematical expectation.

2.2 Calculation of Fatigue Strength under Different Failure Modes

The fatigue limit state functions are established respectively for the three failure modes mentioned above: concrete compressive failure, tensile cracking and reinforcement fatigue fracture. For concrete compressive fatigue, the compressive fatigue strength is taken as the threshold; for tensile fatigue, the limit state equation of tensile stress amplitude and failure cycles is established based on the tensile fatigue strength; for reinforcement fatigue, the fatigue limit state function is constructed according to the material S-N curve.

The specific expression of Song Yupu's concrete tensile fatigue[10] equation is:

$$\lg N_0=16.67-16.76S_{\max}+5.17S_{\min} \quad (10)$$

where: $S_{\max}=\sigma_{\max}/f_{\mathrm{tk}}$, $S_{\min}=\sigma_{\min}/f_{\mathrm{tk}}$, f_{tk} is the tensile strength of concrete under static load.

The compressive fatigue S-N curve of concrete[18] is：

$$S'_{\max}=0.9213-0.0424\lg N_0 \qquad (11)$$

where $S'_{\max}=\sigma_{\max}/f_{\mathrm{ck}}$, f_{ck} is the compressive strength of concrete under static load.

The tensile fatigue S-N curve of prestressed steel[19] strands is：

$$\lg N_0=14.474-3.69\lg\Delta\sigma(N\geq 10^7) \qquad (12)$$

where $\Delta\sigma=\sigma_{\max}-\sigma_{\min}$. According to Equation (10) , the concrete tensile fatigue strength of simply supported beams for heavy-haul railways is:

$$\sigma_{\mathrm{R},Ne}=0.995f_{\mathrm{tk}}+0.308\sigma_{\min}-0.060f_{\mathrm{tk}}\lg N \qquad (13)$$

Combining Equation (9) and Equation (13), the concrete tensile fatigue limit state function of simply supported beams for heavy-haul railways is:

$$G[\mathrm{X},t]_{\mathrm{cp}}=0.995f_{\mathrm{tk}}+0.308\sigma_{\min}-0.060f_{\mathrm{tk}}\lg\left(N_{\mathrm{e,per}}\cdot t\right)-\sigma_{\mathrm{e},t} \qquad (14)$$

Similarly, substituting Equation (11) into Equation (9), the concrete compressive fatigue limit state function of simply supported beams for heavy-haul railways can be expressed as:

$$G[\mathrm{X},t]_{\mathrm{ct}}=0.9213f_{\mathrm{ck}}-0.0424f_{\mathrm{ck}}\lg\left(N_{\mathrm{e,per}}\cdot t\right)-\sigma_{\mathrm{e,c}} \qquad (15)$$

The reinforcement tensile fatigue limit state function of simply supported beams for heavy-haul railways can be expressed as:

$$G[\mathrm{X},t]_{\mathrm{st}}=10^{(14.474-\lg N_0)/3.69}-\sigma_{\mathrm{e,ct}} \qquad (16)$$

2.3 Calculation of Equivalent Constant Amplitude Stress of Structures

The span of concrete simply supported beams for heavy-haul railways is usually 8-32 m (such as the common 24 m and 32 m standard spans), while the length of a single heavy-haul train carriage (such as C80 freight car) is about 12 m. The symmetrical mid-span is selected as the key position (marked with a red dot in Figure 1). The vertical load of a single train acting on the simply supported beam bridge can be equivalently generalized as a combined concentrated load. Figure 1 shows the load layout of a heavy vehicle with 25 t axle load.

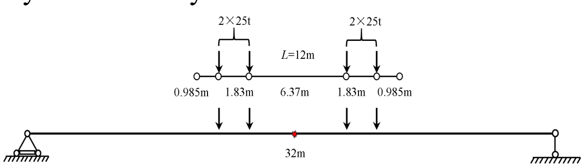

Figure 1. Simplified Model of Train Load

As shown in the schematic diagram of mid-span bending moment of the bridge in Figure 2, the fatigue effect of train loads can be regarded as a fluctuating cycle in stage C and a single peak cycle formed by the coupling of stages A, B, C and D.

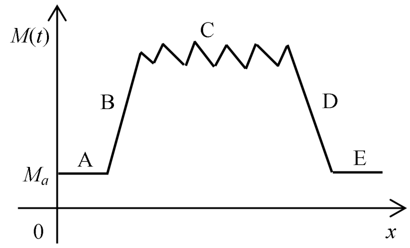

Figure 2. Schematic Diagram of Mid-span Bending Moment Response of the Bridge

Based on the above parameter characteristics of trains and bridges and the load action mechanism, the train load can be quantitatively expressed as the product combination of the axle load parameter T and the impact effect coefficient $(1+\mu)$. In the analysis framework, both the axle load T and the dynamic coefficient μ are treated as random variables. A corresponding load sample combination can be generated by random sampling of the two through Monte Carlo simulation. Using the moving load method and combining with Equation (17), the stress response time history of key components when a train passes through the reinforced concrete bridge for heavy-haul railways can be obtained. After rainflow counting, the equivalent fatigue stress amplitude and the number of stress cycles are obtained by Equation (18)[8]. When the number of samples is sufficient, the probability distribution of equivalent fatigue stress amplitude and cycle times can be fitted. The specific steps of this analysis process are shown in Figure 3.

$$\sigma_{\mathrm{pc}}=\frac{N_{\mathrm{p}}}{A_{\mathrm{n}}}+\frac{N_{\mathrm{p}}e_{\mathrm{pn}}y_{\mathrm{n}}}{I_{\mathrm{n}}}-\frac{\left(\frac{(q_1+q_2)L^2}{8}+M_1\right)y_0}{I_0} \qquad (17)$$

where N_{p} is the effective prestressing force of prestressed tendons; A_{n} is the net section area; e_{pn} is the eccentricity of the resultant force of prestressed tendons to the centroid of the net section; y_{n} is the distance from the centroid of the net section to the calculated position of the section; I_{n} and I_0 are the moment of inertia of the net section and the transformed section of the bridge, respectively; q_1 and q_2 are the dead load intensities of the first and second phases of the T-beam, respectively; L L is the bridge span; y_0 is the distance from the centroid of the transformed section to the tensile edge of the section; M_1 is the bending moment caused by train loads.

$$\sigma_{\mathrm{eq}} = \sqrt[m]{\frac{\sum n_i \cdot \sigma_{\mathrm{a},i}^m}{\sum n_i}} \tag{18}$$

where σ_{eq} is the equivalent stress amplitude.

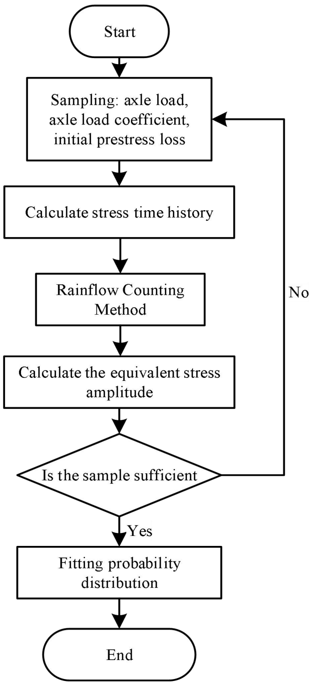

Figure 3. Flow Chart of Equivalent Fatigue Stress Amplitude Calculation

3. Reliability Analysis Method

According to the characteristics of fatigue, the instantaneous failure probability of the structure at time t can be defined as:

$$P_f(T) = \Pr\{G[\mathbf{X},t] \geq 1, \exists t \in [0,T]\} \tag{19}$$

In Equation (19) , $t$is a fixed time point. The instantaneous failure probability can be solved by traditional time-invariant reliability calculation methods, such as Monte Carlo simulation (MCS) method and moment method.

This paper adopts a point estimation method for calculating the statistical moments of performance functions developed by Zhao and Ono[20]. For the performance function $Z = G(\mathbf{X})$ its first k order central moments are defined as:

$$\mu_G = E[G(\mathbf{X})] = \int_{-\infty}^{+\infty} G(\mathbf{X}) f_{\mathbf{X}}(\mathbf{X}) \mathrm{d}\mathbf{X} \tag{20}$$

$$\sigma_G^2 = E\left\{[G(\mathbf{X}) - \mu_G]^2\right\} = \int_{-\infty}^{+\infty} [G(\mathbf{X}) - \mu_G]^2 f_{\mathbf{X}}(\mathbf{X}) \mathrm{d}\mathbf{X} \tag{21}$$

$$\alpha_k \sigma_G^k = E\left\{[G(\mathbf{X}) - \mu_G]^k\right\} = \int_{-\infty}^{+\infty} [G(\mathbf{X}) - \mu_G]^k f_{\mathbf{X}}(\mathbf{X}) \mathrm{d}\mathbf{X} \tag{22}$$

where G($\mathbf{X}$) denotes the performance function; $\mathbf{X}$ is an n-dimensional random vector representing the uncertain parameters in the performance function; $f_{\mathbf{X}}(\mathbf{X})$ denotes the joint probability density function of the random vector $\mathbf{X}$; μ_G and σ_G denote the mean and standard deviation of the performance function; α_{kG} denotes the k-th order central moment.

Using the Gauss-Hermite integration formula[21], the first k order moments of a function of a random variable can be expressed as:

$$\mu_G = \sum_{j=1}^{m} P_j G[T^{-1}(u_j)] \tag{23}$$

$$\sigma_G^2 = \sum_{j=1}^{m} P_j \left\{G[T^{-1}(u_j)] - \mu_G\right\}^2 \tag{24}$$

$$\alpha_{kG} \sigma_G^k = \sum_{j=1}^{m} P_j \left\{G[T^{-1}(u_j)] - \mu_G\right\}^k \tag{25}$$

where m is the number of point estimations; $u_j = \sqrt{2} t_j$ and $P_j = \omega_j \sqrt{\pi}$ denote the estimation points and corresponding weights in the independent standard normal space, respectively. Here, t_j and ω_j denote the integration points and weights of Gauss-Hermite integration, respectively. Five-point (i.e., m=5) and seven-point (i.e., m =7) estimations are commonly used in practical engineering. This paper adopts 7-point estimation, and the estimation points and weights are listed in Table 1.

Table 1 Estimation Points and Weights in Independent Standard Normal Space

Estimation point	Weight
$u_1 = -u_7 = -2.36675941$	$5.48268856 \times 10^{-4}$
$u_2 = -u_6 = -3.75043972$	$3.07571240 \times 10^{-2}$
$u_3 = -u_5 = -1.15440539$	$2.40123179 \times 10^{-1}$
$u_4 = 0$	$4.57142857 \times 10^{-1}$

It can be seen that for a performance function containing n-dimensional random variables[22], if the number of estimation points corresponding to each random variable is m, the total number of estimation points required to calculate the statistical moments of the performance function is m^n.

In the cubic normal distribution, the standardized performance function Z_s can be expressed as a cubic polynomial of the standard normal distribution[23], that is:

$$Z_s = S^{-1}(U) = a_1 + a_2 U + a_3 U^2 + a_4 U^3 \quad (26)$$

Were a_1, a_2, a_3, a_4, denote polynomial coefficients, which are obtained by equating the first four moments of both sides of the equation. For the specific derivation, please refer to Zhao & Lu[14]. To avoid solving linear equations, the following explicit approximate formula can be used to calculate the polynomial coefficients:

$$a_3 = -a_1 = \kappa \cdot h_3,\ \ a_2 = \kappa - 3h_4,\ \ a_4 = \kappa \cdot h_4 \quad (27)$$

Were,

$$h_3 = \frac{5+(35-\alpha_{3G}^2)h_4^2}{9h_0+30-0.8\alpha_{3G}^2}\alpha_{3G},\ \ h_4 = \frac{2h_0}{2h_0+46(1-1/\alpha_{4G}^2)-\alpha_{3G}^2} \quad (28)$$

$$h_0 = \frac{\sqrt{3\alpha_{4G} - 4\alpha_{3G}^2 - 5} - 2}{1-(3\alpha_{3G}^2+1)/\alpha_{4G}^2},\ \ \kappa = \frac{1}{\sqrt{1+2h_3^2+6h_4^2}} \quad (29)$$

Then, the fourth-moment reliability index based on the cubic normal distribution is expressed as:

$$\beta_{4M-C} = -S(-\beta_{2M}, \alpha_{3G}, \alpha_{4G}) \quad (30)$$

By solving the unary cubic equation, the fourth-moment reliability index is obtained as:

$$\beta_{4M-C} = \frac{a}{3} - \sqrt[3]{A} - \sqrt[3]{B} \quad (31)$$

The coefficients in the formula are calculated by the following formulas:

$$\begin{cases} A = -\dfrac{q}{2} + \sqrt{\Delta},\ \ B = -\dfrac{q}{2} - \sqrt{\Delta},\ \ \theta = \arccos\left(\dfrac{-q}{2r^3}\right),\ \ r = \sqrt{-\dfrac{P}{3}} \\ \Delta = \left(\dfrac{p}{3}\right)^3 + \left(\dfrac{q}{2}\right)^2,\ \ p = c - \dfrac{a^2}{3},\ \ q = \dfrac{2}{27}a^3 - \dfrac{ac}{3} - a + \dfrac{\beta_{2M}}{a_4} \\ J_{1s}^* = a_4\left(-2r^3 + \dfrac{2}{27}a^3 - \dfrac{ac}{3} - a\right),\ \ J_{2s}^* = a_4\left(2r^3 + \dfrac{2}{27}a^3 - \dfrac{ac}{3} - a\right) \\ a = \dfrac{a_3}{a_4},\ \ c = \dfrac{a_2}{a_4},\ \ \beta_{2M} = \dfrac{\mu_G}{\sigma_G} \end{cases} \quad (32)$$

The reliability index at each time point can be calculated according to the above method.

4. Engineering Application

Taking the 32m prestressed concrete simply supported T-beam, which accounts for the highest proportion in heavy-haul railway bridges, as the research object, the fatigue reliability research is carried out.

4.1 Engineering Overview

A precast concrete simply supported T-beam for heavy-haul railways with a span of 32 m has a structural height of 2.6 m and a beam width of 2.45 m. In terms of prestressing arrangement, a total of 4 groups of 12 steel strands with 1×7 structure and 15.2 mm diameter, and 5 groups of 8 steel strands with 1×7 structure and 15.2 mm diameter are arranged. The ultimate tensile strength of the high-strength steel wire used is 1860 MPa, and the control stress during tensioning is set to 1357.8 MPa. The concrete strength grade of the beam body is C60. Ordinary stressed steel bars adopt HPB300 steel bars and HRB400 steel bars, and their material properties are implemented with reference to the parameters of corresponding steel bars in current standards. The design service life of this T-beam is 100 years. According to data review, the design value of the dead load intensity of the first phase is 45.325 kN/m, and the design value of the dead load intensity of the second phase is 41.49 kN/m.

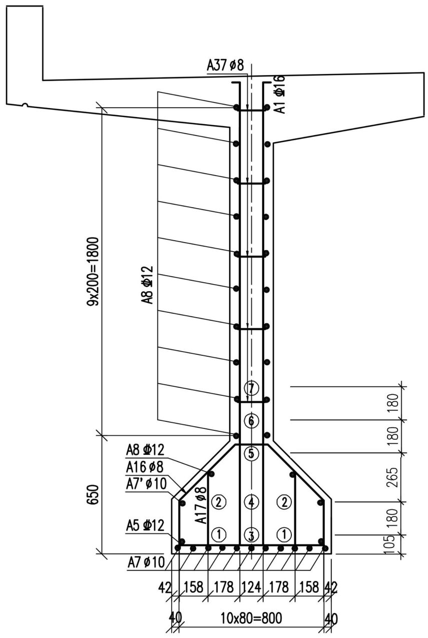

Figure 4. Section Geometric Dimensions and Reinforcement Arrangement

This paper selects the train marshalling with high traffic frequency on heavy-haul railway lines for calculation[24], which consists of 216 C80 heavy-haul freight cars. The calculated length of a single car is 12 m, and the average axle load is N =25t. A single C80 train has a load capacity of 80t, and a full train has a carrying capacity of 17,300t. Referring to the maximum annual traffic volume of a heavy-haul railway of 368 million tons, the daily traffic frequency f_d is converted to about 59 trains. On the basis of analyzing typical working conditions, in order to discuss the influence of single variable changes of train axle load or daily traffic frequency on the research results and the optimal combination, three corresponding working conditions are selected for comparative analysis. A certain railway has an average daily traffic volume of 1.0807 million tons and an average daily operation of 72.1 heavy trains, among which 50.9 are 20,000-ton trains on average daily.

4.2 Distribution Characteristics of Main Random Parameters

This paper mainly follows two principles when selecting random variables: first, they have a significant impact on the fatigue resistance of the bridge; second, they have strong randomness themselves. Based on this, concrete tensile strength, concrete compressive strength, equivalent stress amplitude and the number of stress cycles are all included in the analysis as random variables.

Relevant studies have conducted statistical analysis on the probability distribution information of the selected random variables, and the distribution characteristics are shown in Table 2

At the same time, in the fatigue reliability analysis of concrete T-beams for heavy-haul railways, it can be considered that the train axle load P follows a normal distribution with a mean value of 1.0179P and a standard deviation of 0.0657P; the dynamic coefficient μ follows a normal distribution with a mean value of 0.15 and a standard deviation of 0.06[24]. 100,000 Monte Carlo simulations are carried out by the method in Section 1.3 above to obtain the mean coefficient and standard deviation of the equivalent stress range σ_e, as shown in Figure 5.

In order to balance engineering and calculation, the normal distribution is used to fit the equivalent stress amplitude and the number of actions. The parameters for different parts are shown in Table 2 and Table 3

Table 2. Mean and Standard Deviation of Equivalent Stress Range

Distribution type	Position	Mean value of equivalent stress (MPa)	Standard deviation
Lognormal distribution	Concrete lower flange	0.816	0.00140
	Concrete upper flange	3.837	0.0664
	Steel bar	7.389	0.126

Table 3. Mean and Standard Deviation Value of Stress Cycles

Distribution type	Position	Mean value of equivalent stress	Standard deviation
Lognormal distribution	Concrete lower flange	199.379	2.052
	Concrete upper flange	190.841	3.739
	Steel bar	203.443	0.683

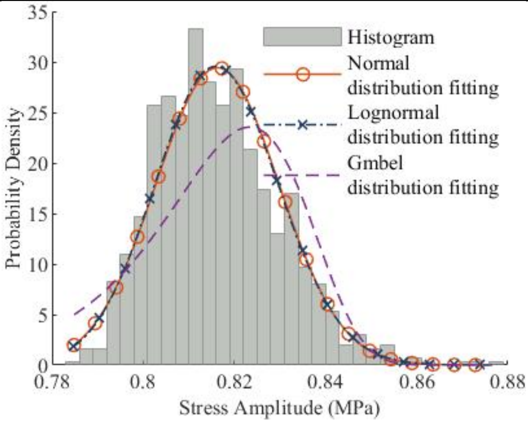

Figure 5. Equivalent Stress Amplitude of Normal Section of Bridge Lower Flange

4.3 Comparative Analysis of Time-varying Reliability under Different Working Conditions

After determining the fatigue limit state function and the values of all variables, the method proposed in this paper is adopted to analyze the fatigue reliability of the bridge within the time span of [0, 100] years. Due to the lack of relevant data, no maintenance or repair is carried out during the 100-year service period. In practice, any maintenance or repair can be considered later by correspondingly adjusting the fatigue damage factors and related reliability indices. When future traffic changes are not considered, the variation curve of the bridge fatigue reliability index with time is shown in Figure 6.

It should be noted that the time-varying reliability of the steel bars of the 32m bridge is extremely high, with a failure probability less than 1.0×10^{-20}, so it is not plotted in the figure. It can be seen from the figure that the compressive fatigue reliability of the upper flange concrete of the bridge is also very high, with a failure probability less than 1.0×10^{-10}. In contrast, the reliability index of the lower flange of the bridge is 4.885 at the initial stage, which is relatively high, but drops to 1.970 at the end of the design service life. For railway bridges, the target reliability index is set at 3.5, and the reliability index of the lower flange drops to 3.341 after 10 years of service. This result indicates that the fatigue problem of the lower flange of the 32m bridge is more serious than that of the steel bars and the upper flange, and maintenance and repair measures are required to extend the service life of the bridge.

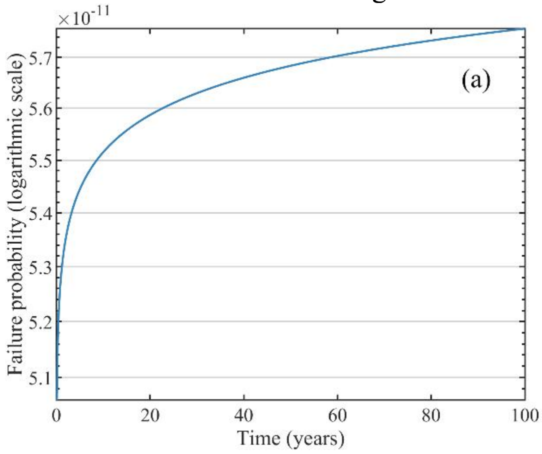

(a) Variation Curve of Fatigue Failure Probability of Bridge Upper Flange with Service Time

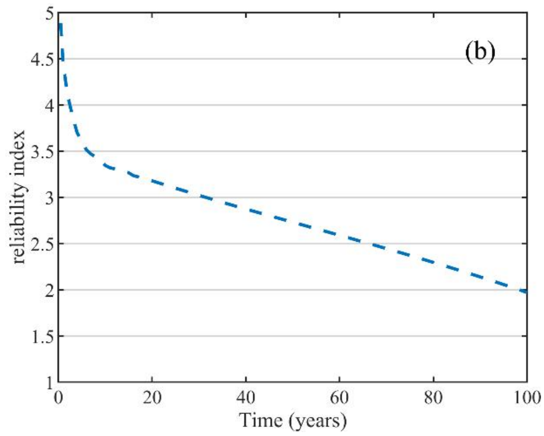

(b) Fatigue Reliability Index of Bridge Lower Flange Versus Service Time

Figure 6. Variation Diagram of Bridge Fatigue Indexes

5. Conclusion

Focusing on the demand for fatigue safety assessment of prestressed concrete bridges for heavy-haul railways, this paper establishes a fatigue limit state function considering the coupling effect of multiple factors and systematically analyzes the evolution law of structural fatigue reliability. The main conclusions are as follows:

(1) In terms of the construction of the limit state function, random variables are selected based on the dual principles of "influence significance" and "own randomness", covering key parameters such as concrete tensile strength, concrete compressive strength, prestressed steel bar tensile strength, initial prestress loss, equivalent stress amplitude and the number of stress cycles. According to the difference in stress characteristics of different parts, it is clarified that the equivalent stress amplitude of the lower flange of the bridge needs to include the influence of prestress attenuation, while the equivalent stress amplitudes of the upper flange and steel bars do not need to be considered, which improves the adaptability of the function to the actual stress state.

(2) The reliability analysis results show that for the 32m concrete bridge, the fatigue failure probability of its prestressed steel bars and upper flange during the service period is less than 1.0×10^{-10}, which has sufficient fatigue safety redundancy. For the lower flange of the bridge, its reliability index is about 4.885 at the initial stage of service, showing a trend of "rapid decline first and then slow attenuation" over time. When serving for 100 years, the reliability index drops to about 1.970. The coupled cumulative effect of fatigue damage and prestress attenuation has a great potential impact on structural safety. It is recommended to intensify the detection and maintenance of the lower flange in the middle and later operation stages.

References

[1] Lu, Z. H., Ma, Y. F., Song, L., & Yu, Z. W. (2017). Experimental study on fatigue behavior of 8 m low-height reinforced concrete plate-girder of heavy-haul railway. *Journal of Central South University (Science and Technology)*, 48, 2550–2558.

[2] Song, L., Cui, C. X., Liu, J. L., & Yu, Z. W. (2021). Corrosion-fatigue life assessment of RC plate girder in heavy-haul railway under combined carbonation and train loads. *International Journal of Fatigue*, 151, 106368. https://doi.org/10.1016/j.ijfatigue.2021.106368.

[3] Yu, Z. W., Li, J. Z., & Song, L. (2014). Experimental study on residual static bearing capacity of heavy-haul railway bridges after fatigue loading. *Journal of the China Railway Society*, 36(4), 76–85.

[4] Giannella, V. (2022). Uncertainty quantification in fatigue crack-growth predictions. *International Journal of Fracture*, 235(2), 179–195. https://doi.org/10.1007/s10704-022-00672-9

[5] Li, J. Z., & Yu, Z. W. (2014). Study on fatigue influence of heavy axle load train on 32m prestressed concrete simply supported T-beam of existing line. *Railway Standard*

Design, 58(10), 56–61.
[6] Darmawan, M. S., & Stewart, M. G. (2007). Spatial time-dependent reliability analysis of corroding pretensioned prestressed concrete bridge girders. *Structural Safety*, 29(1), 16–31. https://doi.org/10.1016/j.strusafe.2006.04.002
[7] Miner, M. A. (1945). Cumulative damage in fatigue. *Journal of Applied Mechanics*, 12(3), A159–A164.
[8] Sonsino, C. M., Baumgartner, J., & Breitenberger, M. (2022). Equivalent stress concepts for transforming of variable amplitude into constant amplitude loading and consequences for design and durability approval. *International Journal of Fatigue*, 162, 106949. https://doi.org/10.1016/j.ijfatigue.2022.106949
[9] Song, L., & Yu, Z. W. (2019). Fatigue damage experiments of heavy haul railway prestressed concrete beams using fiber bragg grating sensing technology. *Journal of Building Structures*, 40(1), 58–66.
[10] Song, Y. P. (2006). *Fatigue performance and design principle of concrete structures*. China Machine Press.
[11] Yang, O., Zhang, X. F., Huo, J. S., et al. (2017). Research status of fatigue performance of prestressed concrete beams. *Journal of Architecture and Civil Engineering*, 34(4), 85–95. https://doi.org/10.1007/s11709-017-0392-7
[12] Wang, Y., Yu, T., Zhang, L., Yin, L., Wu, Y., & Chen, B. (2022). Fatigue performance of rib beam bridge slabs reinforced with polyurethane concrete based on the damage theory. *Buildings*, 12(6), 704. https://doi.org/10.3390/buildings12060704
[13] Zhou, Y., Wang, M., Pan, T., Yang, N., Liu, Y., & Zeng, W. (2026). Interrupting corrosion-fatigue synergism in RC beams: Proactive CFRP intervention via multi-axial anchor confinement. *Structures*, 88, 111981. https://doi.org/10.1016/j.istruc.2026.111981
[14] Zhao, Y. G., & Lu, Z. H. (2021). *Structural reliability: Approaches from perspectives of statistical moments*. Wiley-Blackwell.
[15] Lu, Z. H., Zhang, S. W., Zhang, X. Y., Li, C. Q., Liu, L., & Zhan, J. W. (2024). Time-dependent fatigue reliability analysis of heavy-haul railway steel bridges. *Engineering Structures*, 305, 117737. https://doi.org/10.1016/j.engstruct.2024.117737
[16] Andrieu-Renaud, C., Sudret, B., & Lemaire, M. (2004). The PHI2 method: A way to compute time-variant reliability. *Reliability Engineering & System Safety*, 84(1), 75–86. https://doi.org/10.1016/j.ress.2003.10.005
[17] Peng, J., Chai, Y., Yao, Y., Zhang, J., & Wang, L. (2026). High-Cycle Fatigue Behavior and Fracture Mechanism of Q370qD Bridge Steel Subjected to Different Stress Levels. *Journal of Materials in Civil Engineering*, 38(5), 04026078.
[18] Wu, P. G., Zhao, G. Y., & Bai, L. M. (1994). Study on compressive fatigue performance of high-strength concrete. *China Civil Engineering Journal*, 27(3), 33–40.
[19] Zhang, H., Li, M. Y., Wang, L. H., et al. (2024). Calculation of residual bearing capacity and fatigue life assessment of parallel steel strand stay cables. *Journal of Highway and Transportation Research and Development*, 41(12), 116–127.
[20] Zhao, Y. G., & Ono, T. (2000). New point estimates for probability moments. *Journal of Engineering Mechanics*, 126(4), 433–436. https://doi.org/10.1061/(ASCE)0733-9399(2000)126:4(433)
[21] Zwillinger, D. (2018). *CRC standard mathematical tables and formulas*. CRC Press.
[22] Xu, H., & Rahman, S. (2004). A generalized dimension-reduction method for multidimensional integration in stochastic mechanics. *International Journal for Numerical Methods in Engineering*, 61(12), 1992–2019. https://doi.org/10.1002/nme.1064
[23] Cai, C. H., Lu, Z. H., Xu, J., et al. (2019). Efficient algorithm for evaluation of statistical moments of performance functions. *Journal of Engineering Mechanics*, 145(1), 06018007. https://doi.org/10.1061/(ASCE)EM.1943-7889.0001527
[24] Gao, T. X., Li, Z. S., Zhang, J. W., et al. (2023). Fatigue reliability analysis of RC beams for heavy-haul railways based on direct probability integration method. *Journal of Railway Science and Engineering*, 20(4), 1416–1424.

